Characterizations of Centrifugal Electrospun Polyvinyl Alcohol/Sodium Alginate/Tamanu Oil/Silver Nanoparticles Wound Dressing

Thi Phuong Anh Tran, Anh Hue Luong, and Wei-Chih Lin

***Abstract*— Known for its water solubility, flexibility, strong adhesion, and eco-friendly nature, polyvinyl alcohol (PVA) is widely used in various industries. In the medical field, it is used for applications such as creating bandages and orthopaedic devices. Incorporating sodium alginate (SA) into PVA membranes enhances their structural integrity, breathability, and permeability, thereby minimising the risk of cellular damage in the wound zone. Moreover, the addition of tamanu oil (*Ca*lophyllum inophyllum L.) and silver nanoparticles, both of which are known for their antibacterial properties and benefits in traditional wound healing, further enhances the membranes' wound-healing effectiveness. Following production, the membranes undergo a series of tests designed to evaluate their physical properties as well as their antioxidant and antibacterial capabilities. Subsequently, *i*n vitro testing is conducted using human skin cells; experiments on Wistar rats are then performed. Numerous experiments have consistently demonstrated that the performance of polyvinyl alcohol/sodium alginate/tamanu oil (PVA/SA/Oil) membrane is superior to that of polyvinyl alcohol/sodium alginate/tamanu oil/silver nanoparticles (PVA/SA/Oil/Ag NP) membrane. Specifically, the polyvinyl alcohol/sodium alginate (PVA/SA) combination exhibits an impressive wound-healing rate of 98.82% after 15 days, with cells maintaining a high viability of 92% in a nourishing environment. Moreover, these membranes exhibit exceptional resistance to the oxidation of free radicals, surpassing the 70% threshold, and they possess antibacterial activity against *S*taphylococcus aureus subsp. *a*ureus*i*n vitro. Based on the obtained results, the nanofiber membranes composed of polyvinyl alcohol/ alginate/ tamanu oil, with or without silver nanoparticles, have shown potential as wound dressings in the wound care discipline.**

Manuscript received 3 October 2023; revised 27 November 2023 and 6 February 2024; accepted 15 February 2024. Date of publication 1 March 2024; date of current version 3 April 2024. This work was supported by the National Science and Technology Council, Taiwan, under Grant MOST 110-2221-E-110-066-MY2 and Grant NSTC 112-2221-E-110-034. *(Corresponding author: Wei-Chih Lin.)*

Thi Phuong Anh Tran was with the Department of Mechanical and Electromechanical Engineering, National Sun Yat-sen University, Kaohsiung 804201, Taiwan. She is now with the Food and Biotechnology Institute, Can Tho University, Can Tho 94100, Vietnam (e-mail: Trphuonganh011102@gmail.com).

Anh Hue Luong and Wei-Chih Lin are with the Department of Mechanical and Electromechanical Engineering, National Sun Yat-sen University, Kaohsiung 804201, Taiwan (e-mail: d113020012@student.nsysu.edu.tw; wc.lin@mail.nsysu.edu.tw).

Digital Object Identifier 10.1109/TNB.2024.3371224

***Index Terms*— Centrifugal electrospun nanofiber, polyvinyl alcohol/sodium alginate/tamanu oil, silver nanoparticles (Ag NP), wound healing.**

I. Introduction

BECAUSE numerous factors can hinder the wound-healing process, it is important to develop a better understanding of the factors that affect tissue repair. This understanding will support the identification of the appropriate treatment methods for accelerating wound healing and treating wounds. Among such methods, wound dressing is a crucial factor in wound care. A good wound dressing meets requirements such as the ability to absorb a large amount of fluid, including blood, pus, and other exudates; the ability to keep the wound dry and prevent infection; antimicrobial properties that prevent the spread of bacteria and other pathogens in the wound; and the ability to create favourable conditions for cellular regeneration and tissue remodelling, which accelerate wound healing [1].

Polyvinyl alcohol (PVA) has a wide range of practical applications due to its hydrophilic and biocompatible properties. Polyvinyl alcohol can easily be dissolved in water, can easily be sprayed into fibres in the form of a solution, is chemically resistant, and is physically durable. PVA is used as an adhesive and emulsifier and plays many important roles in the sewing and paper manufacturing industries [2]. Moreover, PVA is praised for its biodegradability, aligning with eco-friendly trends. It is approved for use in several medical applications, including transdermal patches, the creation of jellies that quickly dry on contact with skin, and immediate- and sustained-release pill formulations [3].

Sodium alginate (SA) is a polyelectrolyte that can be used in the manufacturing of various products that benefit life, such as biomaterial sources, bioshells, food-sector applications, cosmetics, textiles, and so on. Artificial alginate fibers may be injected via reasonably stable, tiny holes to produce filaments, which has led to the growing popularity of SA-based solutions. In addition, because alginate fibers accelerate both the cellular-fixation process and wound healing, their potential medical applications have attracted a great deal of attention [4], [5], [6], [7], [8], [9], [10]. Thus, using a combination of PVA and SA membranes is recommended. Whereas SA provides

flexibility, PVA provides stiffness, and this combination of qualities results in the formation of a moderately strong barrier.

Moreover, *Calophyllum inophyllum*L., also known as tamanu or beach calophyllum, is a member of the Clusiaceae (syn. Guttiferae) family [11]. This species is a large evergreen tree that originates from various regions, including Africa, South India, Southeast Asia, Polynesia, the Philippines, and Australia. In traditional medicine, various parts of the *C. inophyllum* plant, including its leaves, bark, fruits, and seeds, have been used to treat numerous diseases [12]. However, the oil extracted from the seeds has been used predominantly in cosmetic and therapeutic applications to address various skin conditions, including burns, dermatoses, eczema, certain skin allergies, acne, psoriasis, herpes, chilblains, skin cracks, diabetic sores, haemorrhoids, dry skin, and hair loss. Tamanu oil has also proved effective in treating conjunctivitis and facilitating the healing of burns and flat wounds [13]. During a phytochemical screening, the compounds present in the plant material were identified. The screening detected the presence of various flavonoids in the oil, including calophyllolide, calophyllic acid, inophyllum B, inophyllum C, and inophyllum E [14]. These compounds are the key components found in tamanu oil, along with polyphenols having antioxidant properties. Together, they contribute to the oil's impressive ability to reduce inflammation, promote healing, and specifically aid in wound healing [15], [16]. Tamanu oil exhibits anti-inflammatory, antioxidant, antibacterial, antiviral, antifungal, photoprotective, and wound-healing activities. Moreover, in the International Nomenclature of Cosmetic Ingredients, tamanu oil is termed "*Calophyllum inophyllum* seed oil" [17].

In the past, the electrospinning technique was a traditional method for the production of nanofiber from polymers. It brings numerous benefits compared to other nanofabrication methods [18]. It aligns with three key directions in nanoscience and engineering: scaling down to picotechnology, achieving enhanced order with diverse nanoarrays, and creating intricate structures such as multi-chamber configurations and nanodevices [19], [20], [21]. The development of complex nanostructures stands out as a significant advancement in this field. For several decades, electrospinning has demonstrated its ability to greatly improve the drug delivery applications of biomolecules by producing medicated nanofibers [18], [20]. On the other hand, the versatility of structural polymeric nanohybrids in various functional applications has garnered significant interest. However, electrospinning typically produces short fibers, which may not be ideal for applications that require long fibers or continuous materials [22], [23]. Additionally, achieving a high degree of fiber alignment can be challenging, which may limit its suitability for certain applications that require precise fiber orientation [22], [24]. Furthermore, the application of electrospinning for large-scale production of nanofibers is restricted due to its low efficiency in the preparation process [24]. Therefore, centrifugal electrospinning (CES) is a revolutionary method that combines centrifugal spinning and electrospinning (ES) to produce nanofibers [24]. Several advantages of the centrifugal electrospinning technique have been reported in preliminary research [24], [25], [26]. This method enables the effective manufacturing of nanofibers with robust bonding based on the use of both centrifugal and electrostatic forces [24]. By using this technique, ultrathin nanofibers could be generated with diameters in the tens of nanometer regime and the productivity of the highly interconnected nanofiber nonwoven meshes was orders of magnitude faster compared to that of materials made with traditional electrospinning methods [26]. The concentration of the polymer, the spinning rate, the operating voltage, and the size of the needle play important roles throughout the manufacturing process [24]. Notably, the presence of residual solvents in the fibres may be effectively addressed by the CES method if a molten polymer is employed as a precursor [24], [25]. In recent years, scientists have been exploring how tiny nano and microfiber frameworks can aid in healing wounds, regenerating tissue, and protecting the skin [27]. The fibers that are created through this process are exceptionally well-suited for various healthcare applications, such as crafting frameworks for tissue engineering, creating solid dispersions for delivering medications, producing antimicrobial meshes for filtration purposes, and developing bandage-like fibrous coverings for wound care [27], [28]. The significant potential of these advancements, as well as their future developments, underscores their importance in the field of biomedical research and application.

The primary objective of this study is to investigate the effectiveness of PVA and SA nanofiber biomembranes in facilitating wound healing *in vivo*. To enhance the healing capabilities of the developed membrane, tamanu oil was integrated into the mixture of the membrane solutions. Additionally, in an effort to bolster the PVA/SA membrane's healing properties, tamanu oil and nanosilver were introduced into the aqueous membrane solution used to create the antioxidant and antibacterial biomembranes. Before the animal experiment was conducted, the quality of the membrane was thoroughly evaluated through a set of *in vitro* assessments that comprised physical tests as well as tests of resistance to oxidation, antibacterial activities, and cell viability. These evaluations could serve as the foundation for developing products that support the process of healing both human and animal wounds.

II. Materials and Methods

A. Chemicals

This study employed the following chemicals: polyvinyl alcohol (Sigma-Aldrich), sodium alginate (Sigma-Aldrich), tamanu oil (Thai Duong, Vietnam), 2,2-diphenyl-1-picrylhydrazyl (DPPH; Sigma-Aldrich), fetal bovine serum (Sigma-Aldrich), ethanol (C_2H_5OH), trypsin (Sigma-Aldrich), Dulbecco's modified eagle medium (Sigma-Aldrich), phosphate buffer solution (Sigma-Aldrich), L-ascorbic acid (Sigma-Aldrich), and silver nitrate ($AgNO_3$; Sigma-Aldrich), cell counting kit-8 (CCK-8) (Sigma-Aldrich), penicillin-streptomycin solution (Sigma-Aldrich).

B. Preparation of PVA and SA Nanofiber Membranes

The membrane isolation and vesicle production were conducted following the methodology outlined by [24] and [29],

although with minor modifications. To prepare solutions with a 20% PVA concentration, PVA was dissolved in distilled water at 90°C for 5 hours under continuous stirring. To yield distinct sample variations, a mixture was then prepared by incorporating either 20% tamanu oil or a combination of 20% tamanu oil and 20% nanosilver (Ag NP). Additionally, SA was dissolved in distilled water and blended to a 2% solution (weight percentage) for 1 hour at 30°C. The resulting SA solution was then vigorously mixed with PVA at a 7:3 ratio while maintaining room temperature. Stirring was continued for 30 minutes at 30°C to ensure complete dissolution of the PVA and SA. The resulting solution was loaded into a 5-mL glass syringe and positioned within a holder, which was propelled by a pump to enable a steady flow rate. The solutions entered the electric field, which was created with an adjustable voltage source, after flowing from the syringe through the blunt-tipped stainless steel needle. The needle was fastened to a holder that could move forward in front of the mandrel. A ground-collecting plate composed of aluminium foil was located 6 cm from the needle tip as specified. On the aluminium-foil-covered revolving mandrel, the remaining polymer chains that make up the nanofibrous mats were gathered. A variable speed was used for the mandrel's rotation. The CES process was conducted at ambient temperature, employing high voltages of 12 kV and mandrel-rotation speeds of 1300 rpm. Subsequently, the nanofibers collected on the aluminium foil were stored at room temperature for use in the characterisation studies. The samples were signed as PVA/SA, PVA/SA/Oil, PVA/SA/Oil/Ag NP.

This study's process of synthesising silver nanoparticles involved adapting the original method of [30]. Using double distilled water, two solutions were prepared, one with a 1% concentration of silver nitrate and the other with a 1% concentration of L-ascorbic acid. These solutions were then mixed in varying proportions and subjected to sonication in a dark environment at a temperature of 25°C for 20 minutes. The formation of silver nanoparticles was confirmed by the presence of a golden-yellow colour and the absorption of light at a wavelength of 300–500 nm by using a UV-Vis spectrophotometer (Jasco V-730, Japan). Further investigation showed that a stable, golden-yellow colour was achieved when the concentrations of silver nitrate [30], [31], [32], [33]. Additionally, synthesized silver nanoparticles were observed under an analytical scanning transmission electron microscope (TEM, JEOL 3010).

The morphology of the nanofiber membranes was analyzed using high-resolution scanning electron microscopy (SEM, Zeiss GeminiSEM 450) with a 3 kV accelerating voltage. Prior to observation, all samples underwent dehydration and were coated with a thin layer of gold. The diameter of the fabricated nanofibers was assessed using Oxford software.

C. Mechanical Properties

The properties of tensile strength were evaluated with tensile testing. A tensile machine (FGS-50E-H, Nidec-SHIMPO, Japan) was employed to investigate the tensile strength and elongation of the hydrogel. The tensile properties were evaluated by stretching the samples to break at a crosshead speed of 20 mm/min. The initial cross-sectional area (10 mm^2) was used to calculate the tensile strength. The test was repeated four times to report for each sample at room temperature.

PVA-concentrated biomembrane samples were dried at 105°C until the weight was constant. Subsequently, the dry sample was soaked in water that had been kept at 37°C, and the volume change was measured until it stopped rising. The following formula was used to determine the membrane's degree of swelling [34], [37]:

$$\%\text{Swelling degree} = \frac{W_t - W_d}{W_d} \times 100, \tag{1}$$

where W_t is the membrane's mass after being submerged in water and W_d is the dried membrane's mass.

D. Cell-Proliferation Assay

For this cell-proliferation experiment, the CCK-8 was used. It computes the number of living cells in the cell-proliferation experiment using a sensitive colourimetric assessment of the solution response [35]. WST-8 or [2-(2-methoxy-4-nitrophenyl) - 3 - (4-nitrophenyl) - 5 - (2,4 disulfophenyl) - 2H - tetrazolium, monosodium salt] was reduced by dehydrogenases in cells to form a yellow product (formazan) that was soluble in the tissue-culture medium. The detection sensitivity of CCK-8 is higher than that of other tetrazolium salts, such as MMT, XTT, MTS, and WTS-1 [36]. Plate cells per well in a tissue-culture microplate with a clear bottom. The cells were seeded onto the samples fixed in the 24-well plate and incubated in a 37°C, 5%-CO_2 incubator. After 48 hours, a working solution composed of medium and 10% CCK-8 reagent was prepared to assess cell viability. For the blank well (containing the medium without cells), an equivalent amount of CCK-8 was added. The volume of the working solution is 100 μL for a 96-well plate. The solution was protected from the light and incubated in a 5%-CO_2 incubator for 2.5 hours at 37° C. The increase in absorbance was measured at 450 nm by using a microplate reader (Bio-Rad 680, Bio-Rad, USA) [37]. The following formula was used to determine the cell-viability rate:

$$\%\ cell\ viability = \frac{\text{As} - \text{Anc}}{\text{Apc} - \text{Anc}} \times 100, \tag{2}$$

where Anc is the absorbance of the negative control, Apc is the absorbance of the positive control, and As is the absorbance of the sample.

E. Antioxidant Assay

This assay was based on the theory that a hydrogen donor is an antioxidant DPPH is one of the few stable and commercially available organic nitrogen radicals. The antioxidant effect is proportional to the disappearance of DPPH in test samples [38]. DPPH was dissolved in ethanol 99% with the necessary reaction concentration of 0.001 mg/mL. A 500-μL sample was added to inhibit a constant volume of 500 μL DPPH solution. Before letting the mixture sit at room temperature in the dark for an hour, vortex it to create a homogenous mixture. The absorbance of this mixture was measured at

517 nm. The proportion of DPPH inhibition was calculated with the following equation:

$$\%Inhibition = \frac{\mathrm{Ac} - \mathrm{Ax}}{\mathrm{Ac}} \times 100, \tag{3}$$

where Ac is the absorbance of the control and Ax is the absorbance of the reaction mixture.

F. Antibacterial Assay

The antibacterial activity of the scaffolds was evaluated using the diameter of the antibacterial against *Staphylococcus aureus* subsp. *aureus* and *Escherichia coli* as representative gram-positive and gram-negative bacteria, respectively. *S. aureus* subsp. *aureus* and *E. coli* were provided by the Bioresource Collection and Research Center, Taiwan. The bacteria were grown overnight in nutrient agar to acquire isolated colonies and then diluted to a viable bacterial suspension containing approximately 10^8cells/mL [36]. Measuring the optical density at 600 nm enabled a calculation of the growth rate and bacterial concentration [39]. Subsequently, 100 μL of the bacterial suspension was spread onto the nutrient agar, then put the membranes onto the surface and allowed to grow for 24 hours at 37°C. The bacterial viability was measured to determine the antibacterial effect of the scaffolds. To test the antibacterial property, five membrane samples were used: PVA/SA, PVA/SA/Oil, PVA/SA/Oil/Ag NP, and Oil/Ag NP. To test positively, a penicillin-streptomycin solution 0.5 mg/ml was used. To test negatively, nothing was utilised. The inhibitory effect of each sample was measured by determining the diameter of the zone of inhibition, which indicates the area where bacterial growth is prevented. The diameter of the antimicrobial "halo" was calculated as follows [40]:

$$C = \mathrm{D} - \mathrm{d} \tag{4}$$

where C is the bridging of the zone of inhibition (cm), D is the susceptible zone (cm), and d is the diameter of the sample disk (cm).

G. Wound-Healing Assay

Experiments were conducted on male Wistar rats aged 8 weeks and weighing 200–250 g that were provided by BioLasco, Taiwan. The experiment was conducted under the approval of the Institutional Animal Care and Use Committee of the National Sun Yat-sen University, Kaohsiung, Taiwan (IACUC Approval No. 10738). The rats were adapted to the experimental environment over the course of five days. Food and water were provided during the experimental period. The rats were divided into five groups with five mice/group as follows: the control group was treated with normal saline and commercial povidone iodine, one group was treated with PVA/SA membrane, one group was treated with PVA/SA/Oil membrane, one group was treated with PVA/SA/Oil/Ag NP membrane, and one group was treated with tamanu oil and nanosilver-loaded bandage. A wound with a length of 2–2.2 cm was created on the back of each mouse. The wound status and wound size were recorded periodically over the course of 15 days [34]. The percentage of wound healing was assessed with the following equation:

$$\%Healing = \frac{W0 - Wx}{W0} \times 100, \tag{5}$$

where $W0$ is the wound area at day 0 and Wx is the wound area at day 3, 6, 9, 12, and 15.

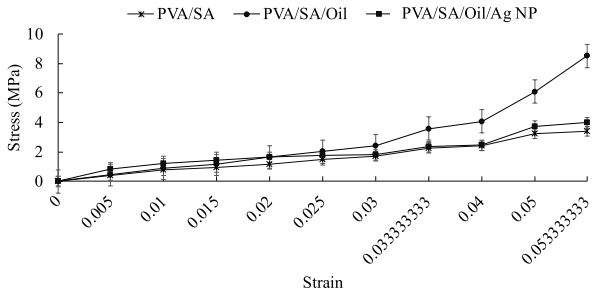

Fig. 1. Stress–strain curve of the PVA/SA, PVA/SA/Oil, and PVA/SA/Oil/Ag NP nanofiber membranes.

H. Histology

The assessment of the histological condition involved evaluating the extent of inflammation, re-epithelialization, and the formation of granulation tissue in the tissue sections. The histological study of the wound treated with the samples, which occurred on day 15, involved the euthanasia of the rats. Subsequently, wound tissue samples of all treatments, including a 5 mm border of adjacent normal skin, were carefully collected for histological analysis. The harvested tissues were initially fixed in a 4% paraformaldehyde solution for a duration of 6 hours. Following this, the samples were cut along the widest margin and immersed in the fixing solution overnight. The processed tissue samples underwent a series of procedures, including dehydration, diaphanization, wax infiltration, and embedding in paraffin. To evaluate the status of the newly regenerated tissues concerning the treatment administered, the paraffin-embedded tissue samples were sectioned into 5 μm thick slices and subjected to staining with hematoxylin and eosin (H&E). For the qualitative histological analysis, a digital slide scanner (MoticEasy-Scan, Hong Kong) was employed to facilitate microscopic observations [34].

1) Statistical Analysis: All groups were compared using a one-way analysis of variance (ANOVA) via Tukey's factor test. Each experiment was run at least three times in duplicate, and the results were reported as means ± standard deviations (SD). A confidence interval was calculated and a significant difference was highlighted with ∗∗ denoting a p value ≤ 0.05.

III. Results and Discussion

A. Mechanical Properties

The membranes to various tests to evaluate their physical properties, such as tensile strength and swelling behaviour. Fig. 1 illustrates the stress–strain curves of three types of membranes: PVA/SA, PVA/SA/Oil, and the PVA/SA/Oil/Ag NP membrane. The chart shows that the PVA/SA/Oil membrane exhibited a superior stress–strain curve compared to

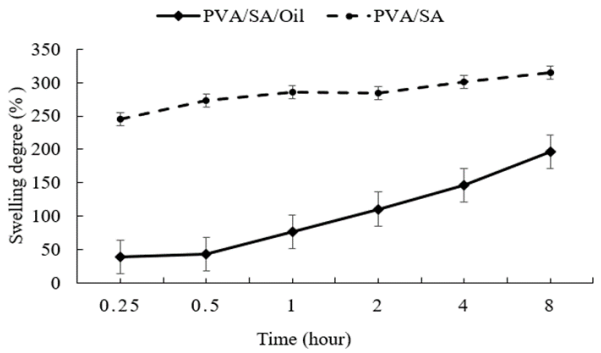

Fig. 2. Degree of swelling of the PVA/SA and PVA/SA/Oil nanofiber membranes.

both the PVA/SA membrane and the sample incorporating nanosilver and tamanu oil (PVA/SA/Oil/Ag NP). Specifically, in the strain range of 0.03–0.053, the PVA/SA/Oil membrane reached a stress value of over 8 MPa, while the other samples only showed slight increases without surpassing 4 MPa. The higher stress value for the PVA/SA/Oil nanofiber membrane suggests that the addition of oil to the PVA/SA material might have improved its mechanical properties. It also indicates that this membrane can withstand higher levels of mechanical deformation. Besides, the swelling behaviour of the PVA/SA membranes was observed in both the presence and absence of tamanu oil. The membranes were immersed in water, and water-uptake capacity was monitored over an 8-hour period, as shown in Fig. 2, the PVA/SA/Oil samples exhibited slower and reduced swelling compared to the PVA/SA samples, showing a threefold difference. These results indicate that the PVA/SA/Oil membrane has better water permeability and mechanical properties, such as flexibility, resilience, and strength. Therefore, both the PVA/SA and PVA/SA/Oil membranes are believed to provide an improved wound healing process by effectively absorbing blood, pus, and wound exudates, protecting the wound against harmful agents, and maintaining a humid micro-environment around the wound.

B. Morphology of Nanofiber Membranes

The fabrication of nanofiber membranes using the CES method allows for the production of membranes with consistent fiber diameter, and long fibers. In Fig. 3A, it can be observed that the fibers in both the PVA/SA/Oil and PVA/SA membrane samples ranged predominantly from 100 to 300 nm. These dimensions are substantially smaller when compared to the 400 to 1800 nm diameter of fibers typically produced using identical methods, as catalogued in [29], [33], and [41]. Furthermore, they are also less than the mean diameter of PVA/SA membranes — 365.8 nm, as procured via the electrospinning technique according to [42]. The scanning electron microscope (SEM) images provided in Fig. 3B shows that the fibers in the PVA/SA and PVA/SA/Oil membranes largely share a similar morphology. They manifest as extended, uninterrupted fibers that wind around one another and pile up layer by layer until the desired thickness is achieved. However, in the case of the PVA/SA membrane combined with tamanu oil, it can be observed that the resulting fibers

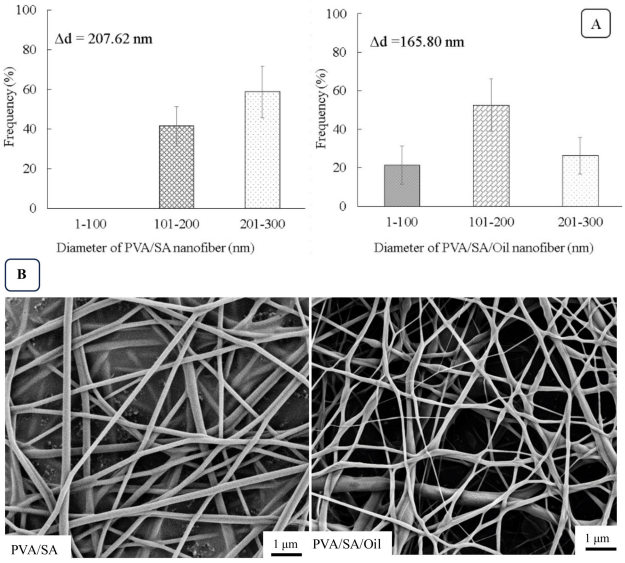

Fig. 3. The diameter distribution of PVA/SA and PVA/SA/Oil membranes respectively (A), and the fiber morphology of these membranes under a Scanning Electronic Microscopy (SEM) of PVA/SA and PVA/SA/Oil membranes respectively (B).

exhibit uneven sizes unlike the fibers in the PVA/SA membrane without tamanu oil. An interesting observation with this approach is that a considerable number of void spaces form within the membrane structure. This imparts a certain porosity and breathability to the membrane, an attribute that is advantageous in fostering a conducive environment for wound healing [43]. These findings correspond with the swelling degree of each sample. Furthermore, the addition of oil in the PVA/SA/Oil membrane made the inner material somewhat impermeable, resulting in slower swelling capability compared to the PVA/SA membrane. These insights indicate that the nanofiber membranes possess the capacity to absorb exudates secreted by damaged blood vessels in injured tissue, while also inhibiting the ingress of external agents. This creates an environment that not only prevents bacterial growth but also maintains the necessary humidity for effective wound-care management. In summary, the CES method enables the production of nanofiber membranes with consistent fiber diameter and long fibers. These unique properties allow the nanofiber membranes to effectively absorb exudates and create a better wound-care micro-environment [23].

The characterizations of the synthesized silver nanoparticles are illustrated in Fig. 4. To ascertain the emergence of nano-sized silver formation, an analysis of the UV-Vis absorption spectrum, ranging from 300 to 500 nm of the sample solution, is presented in Fig. 4A. The absorbance linked to surface plasmon resonance is notably sensitive to the characteristics of the surrounding medium and particles, encompassing their nature, size, and shape. In the UV-Vis absorption spectrum of the sample, a distinct peak is observed at approximately 418 - 420 nm, signifying the formation of silver nanoparticles [44]. Subsequently, the silver particles were examined using TEM and EDS analysis, as depicted in Fig. 4B and 4C. The shape of silver particles is spherical, with an average diameter of around 50 nm. These findings align with previous

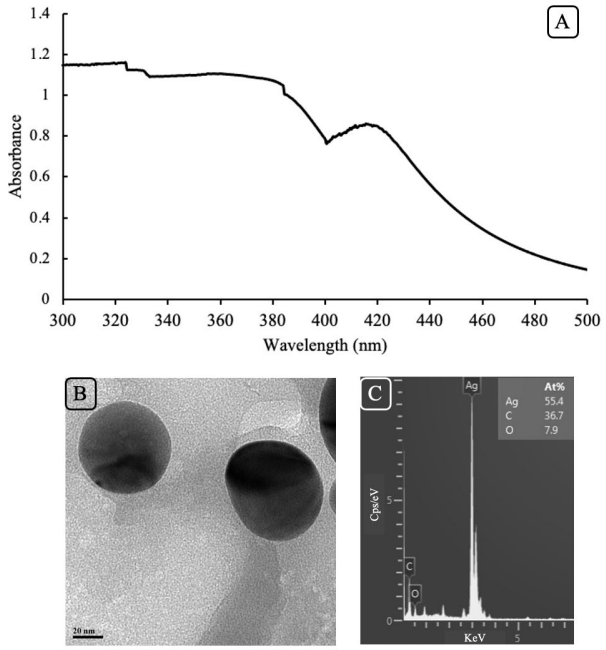

Fig. 4. Analysis of synthesized silver nanoparticles (Ag NP). (A) UV-Vis spectroscopy of Ag NP solution from 300 to 500 nm, (B) image of silver nanoparticles under a Transmission Electron Microscopy (TEM), and (C) Energy-dispersive X-ray Spectrum of Ag NP.

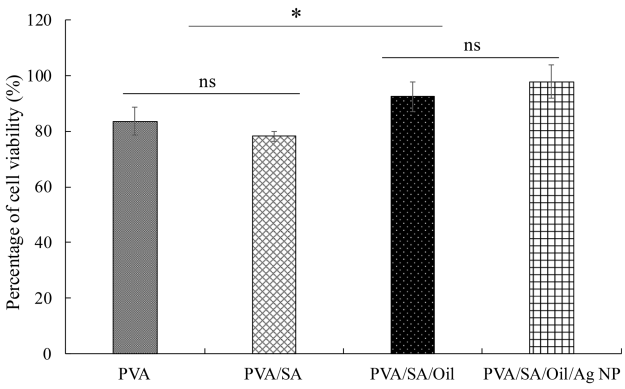

Fig. 5. Percentage of cell viability of the PVA/SA, PVA/SA/Oil, and PVA/SA/Oil/Ag NP membranes, $n = 8$, $p \leq 0.05$, (*) means correlation is significant at the 0.05 level, (ns) means correlation is nonsignificant at the 0.05 level.

studies [44], [45]. The EDS chart of the particles showcases the appearance of silver (Ag - 55.4%), carbon (C - 36.7%), and oxygen (O - 7.9%) in the sample solution, confirming that the observed particles are silver [44].

C. Cell Viability

To assess cell viability, an experiment was conducted on human dermal fibroblast (HDF) skin cells using the CCK-8 [33]. This test evaluated cell viability with the PVA/SA membrane and with a combination of the PVA/SA/Oil and PVA/SA/Oil/ Ag NP membranes under in vitro conditions. The results presented in Fig. 5 show that the cell viability of PVA and PVA/SA membranes reaches around 80% of the cells survived, with the PVA/SA membrane at approximately 77%, and the PVA membrane at approximately 81%. In the PVA/SA/Oil and PVA/SA/Oil/ Ag NP groups, this percentage increased to over 90%, suggesting better cell viability in a nutritionally complete environment. These results demonstrate that supplementing tamanu oil and nanosilver into the PVA/SA membrane did not affect HDF cell growth. In other words, the fabricated nanofiber membranes exhibit excellent biocompatibility. This is a crucial factor in various biomedical applications, such as tissue engineering and drug delivery systems. A previous experiment found that 80% of HDF cells could survive on fabricated scaffolds using PVA membranes [43].

D. Antioxidant-Capacity Assessment Using the DPPH Method

As is well-known, in antioxidant experiments, the higher the percentage of inhibition, the stronger the antioxidant capacity, and vice versa. The antioxidant capacity of the membranes was assessed using the DPPH method, which is presented in the chart in Fig. 5. The obtained results undeniably support the assertion that all three samples showcased compelling antioxidant activity, with percentages surpassing 70%. These membranes possess good antioxidant activity due to their content of alginate, tamanu oil, and silver nanoparticles, all of which have demonstrated effective antioxidant activity in previous studies. For instance, sodium alginate isolated from Tunisian brown seaweed exhibited a scavenging DPPH radical activity of 74% at 0.5 mg/mL [46]. In another study, the antioxidant effectiveness of tamanu oil was evaluated and recorded, showing a strong inhibition of DPPH [47]. Moreover, silver nanoparticles, synthesized using plant extract containing ascorbic acid and polyphenols, demonstrated robust antioxidant resistance [44]. Hence, the PVA/SA, PVA/SA/Oil, and PVA/SA/Oil/Ag NP nanofiber membranes could be used as an antioxidant biomaterial in biomedical engineering applications, especially for skin wound dressing. There is a close connection between chronic skin inflammation and reactive oxygen species in the wound healing process. Reactive oxygen species (ROS), also known as oxidative agents, including superoxide (O^{2-}) and hydrogen peroxide (H_2O_2), are excessively produced in the inflammation stage of the wound [48]. Therefore, the scavenging of ROS, termed antioxidant activity, is an important step to decrease inflammatory reactions in wound healing [1]. By effectively scavenging free radicals, the enhanced protection afforded by these membranes will play a pivotal role in mitigating the risk of infection and minimizing the loss of important cellular components. This, coupled with the ability of nanofiber membranes to scavenge free radicals and provide superior protective properties, underscores their potential as an advanced and promising approach in wound care management.

E. Antibacterial Effectiveness

The results presented in Fig. 7 provide a comparison between the antibacterial effectiveness of the PVA/SA biopolymer nanofiber loaded with tamanu oil and nanosilver and that of commercial antibiotics. In this experiment, the biopolymer fibers were tested for their ability to inhibit the growth of two types of bacteria, *S. aureus* subsp. *aureus*(Gram-positive

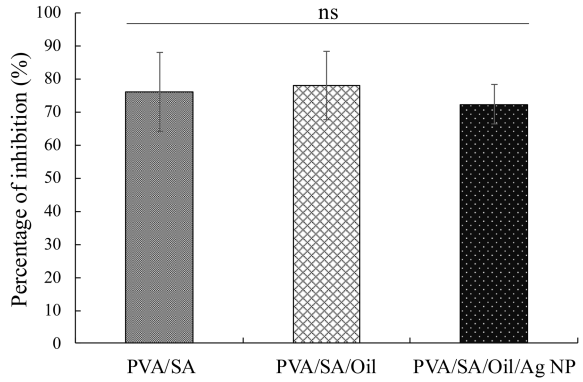

Fig. 6. Antioxidant potential of the PVA/SA, PVA/SA/Oil, and PVA/SA/Oil/Ag NP membranes, $n = 5$, $p \leq 0.05$, (ns) means correlation is nonsignificant at the 0.05 level.

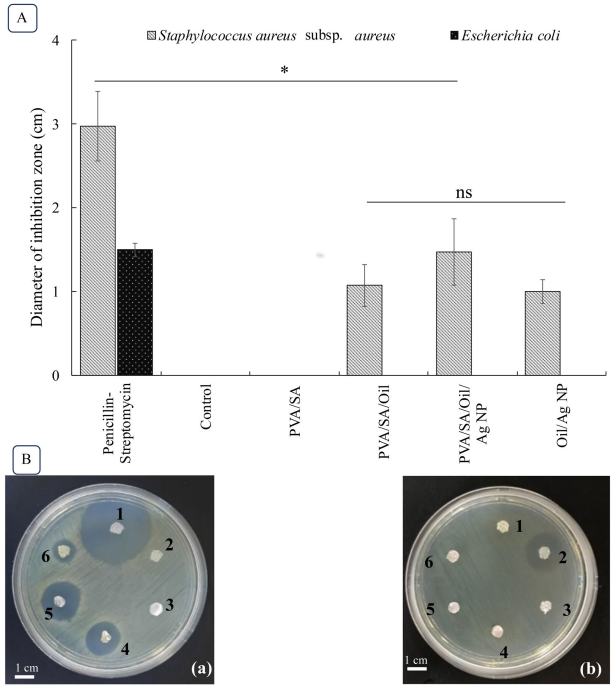

Fig. 7. The antibacterial testing aimed to determine the inhibitory effect (by measuring the diameter of inhibition) of penicillin-streptomycin solution 0.5 mg/mL (1), control (normal bandage) (2), the PVA/SA membrane (3), the PVA/SA/Oil membrane (4), the PVA/SA/Oil/Ag NP membrane (5), and the Oil/Ag NP membrane (6) against the growth of (a) *S*taphylococcus aureus subsp. *a*ureus and (b) *E*scherichia coli, n=4, $p \leq 0.05$, (∗) means correlation is significant at the 0.05 level, (ns) means correlation is non-significant at the 0.05 level.

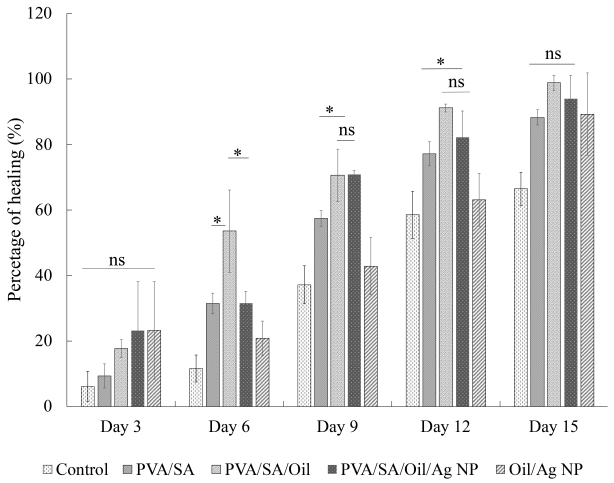

Fig. 8. Percentage of healing in rats at 3, 6, 9, 12, and 15 days, n = 4, $p \leq 0.05$, (∗) means correlation is significant at the 0.05 level, (ns) means correlation is nonsignificant at the 0.05 level.

bacteria) and *E. coli* (Gram-negative bacteria). Regarding the inhibitory effect against Gram-positive bacteria, the PVA/SA biopolymer membrane loaded with tamanu oil and nanosilver exhibited significant efficacy. In comparison with a penicillin-streptomycin solution of 0.5 mg/mL (a positive control), the inhibitory zone of the PVA/SA/Oil/Ag NP membrane on the growth of *S. aureus* subsp. *aureus* is notably effective, approximately 0.5 times larger. Following this, the inhibitory zone of the PVA/SA/Oil membrane (0.36 times larger). The Oil/Ag^{+}-loaded bandage is 0.32 times larger, compared to the positive control. *S. aureus* subsp. *aureus*, a common resident bacterium on the skin and a cause of infections and skin diseases, was selected as a representative Gram-negative bacterium to test antibacterial activity in the study. Infections by pathogenic bacteria are crucial issues in the wound healing stage, and avoiding them is essential to prevent complications after surgery [49]. To effectively protect the wound, antibacterial biomembranes are of research interest. The antimicrobial effectiveness of the biomembranes containing tamanu oil or silver nanoparticles in previous research is also mentioned in [50] and [51], demonstrating the biomembranes' ability to inhibit the growth of Gram-positive bacteria, specifically *S. aureus* subsp. *aureus*. In this study, due to the supplementation of tamanu oil and silver nanoparticles – potent compounds for antibacterial activity – it is proven that the membranes possess good antibacterial activity against *S. aureus* subsp. *aureus*. However, the assessment of the inhibitory effect against Gram-negative bacteria demonstrated that the PVA/SA biopolymer fibres loaded with tamanu oil and nanosilver did not have an inhibitory effect. It is not recorded the inhibitory effect against *E. coli* (Gram-negative bacteria) of all treatments, including the PVA/SA, PVS/SA/Oil, PVA/SA/Oil/Ag NP, and Oil/Ag NP membranes. Gram-negative bacteria generally possess high levels of resistance and are rather difficult to treat with antibiotics. Therefore, to explore the antibacterial potential of the biopolymer fibres made from PVA/SA against other Gram-negative bacteria, further research is needed.

F. Wound Healing

The results of the experiment on wounds in mice treated with PVA/SA, PVA/SA/Oil, and PVA/SA/Oil/Ag NP membranes were compelling and reliable. As Fig. 8 illustrates, the wound-healing capability of the membrane and the effectiveness of incorporating tamanu oil and nanosilver was clearly evident in a comparison with the control sample – which did not use any wound-healing aids. With sample 2 (PVA/SA), the wound had dried and healed faster than with the other samples after 15 days of observation, although it did so more slowly than with samples 3 (PVA/SA/Oil) and 4 (PVA/SA/Oil/Ag NP). Throughout the monitoring process, samples 3 and

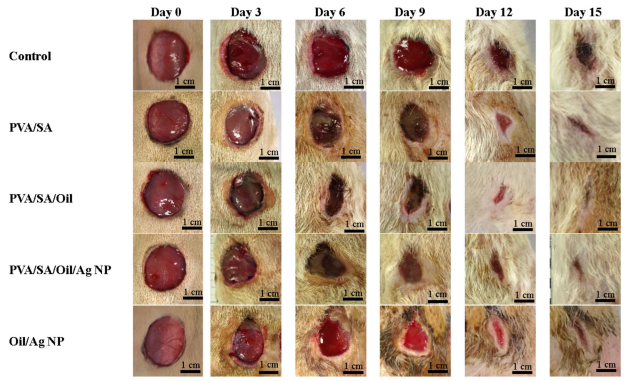

Fig. 9. Wound area of rats at day 0, 3, 6, 9, 12, and 15 after using the PVA/SA, PVA/SA/Oil, PVA/SA/Oil/Ag NP, and Oil/Ag NP membranes and control.

4 exhibited faster blood drying and a faster reduction in wound diameter than did sample 2. Notably, after 15 days of observation, the wound diameter was smaller than that associated with sample 2. Regarding sample 5 (Oil/Ag NP), which served as a positive control in the experiment, in the first 3, 6, and 9 days of observation, the wound drying was slow and accompanied by some bleeding, and the healing effect was not particularly convincing. However, by day 15, sample 5 exhibited good results, with a smaller wound opening compared to the other samples. These results clearly indicate that PVA/SA in combination with tamanu oil and nanosilver has the potential to heal wounds and promote the healing process. However, further research and testing are needed to evaluate the effectiveness and persuasive nature of this approach in wound treatment.

Fig. 9 offers an in-depth analysis of the pace of wound healing for the five experimental treatments over a span of 15 days. It is evident that the wound treated with sample 3 (PVA/SA/Oil) had entirely recuperated, in contrast to the wounds associated with sample 2 (PVA/SA) and 4 (PVA/SA/Oil/Ag NP), which had yet to fully heal. Interestingly, the size of the wounds associated with sample 1 (control) and 5 (Oil/Ag NP) on day 15 was somewhat similar to that of the wound associated with sample 3 on day 12. Ultimately, the healing outcomes depicted in Fig. 8 and 9 underlined the superior performance of the PVA/SA/Oil membrane relative to that of the other samples.

G. Histology

As Fig. 10 shows, all the treatments (PVA/SA, PVA/SA/Oil, PVA/SA/Oil/Ag NP, and Oil/Ag NP) resulted in a full recovery of the epidermis and dermis, whereas the control treatment did not result in a fully reconstitute epidermis. In normal skin, the epidermis layer plays a crucial role as a protective barrier against factors from the external environment such as microorganisms, viruses, and other pathogenic factors [49]. Therefore, the reorganisation of the epidermis layer of wounded skin is necessary. The results demonstrated that the epithelial layer of the injured skin treated with PVA/SA nanofiber, PVA/SA/Oil nanofiber, and PVA/SA/Oil/Ag NP nanofiber not only recovered faster than that in the control sample (without treatment) but also showed fully the structure of skin. At least

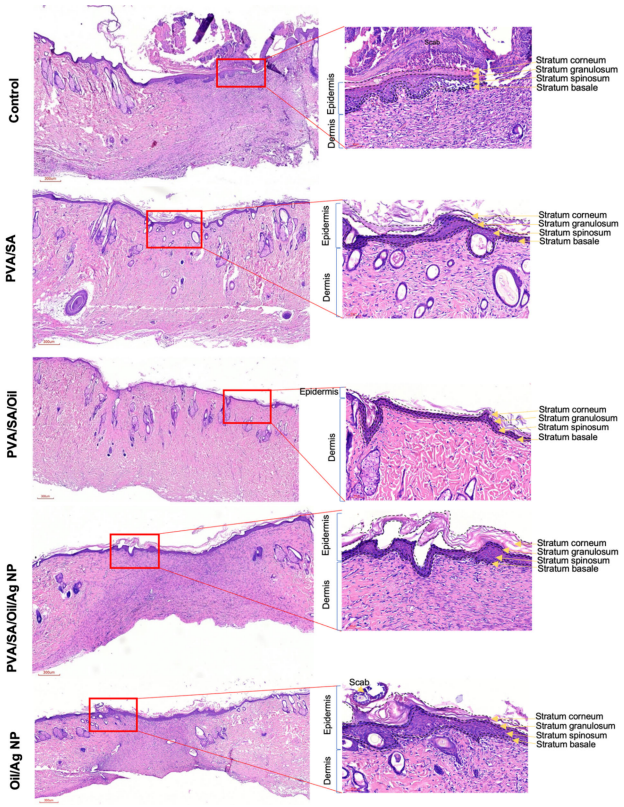

Fig. 10. Histology of the wound zone treated with various samples at day 15 after dual staining with haematosin & eosin (H&E) dye.

two fundamental skin layers (the epidermis and dermis) were observed on the damaged skin treated with PVA/SA nanofiber, PVA/SA/Oil nanofiber, and PVA/SA/Oil/Ag NP nanofiber. It consists of four layers: the stratum corneum, stratum granulosum, stratum spinosum, and stratum basale [52]. These layers are key components in the formation of the epidermis. As a result, the complete epidermis is covered entirely the wound zone in the groups treated with the PVA/SA, PVA/SA/Oil, and PVA/SA/Oil/Ag NP nanofiber membranes. That is, all the samples had the capacity to enhance the wound-healing process.

Fig. 11 illustrates the histological examination of the wounds after 15 days of treatment with the samples. When a skin wound occurs, the body's initial response is the formation of a blood clot to prevent excessive bleeding. This is followed by inflammatory reactions in which various inflammatory cells, such as neutrophils, eosinophils, lymphocytes, and macrophages, are released to absorb antigens. In response to a skin injury, the body immediately activates the immune mechanism and initiates the reconstruction of damaged skin [53]. The results indicate that the inflammation stage was prolonged in this group. In other words, the healing process was incomplete after 15 days. Inflammation is a biophysical reaction that involves the recruitment of immune cells, such as neutrophils, lymphocytes, and macrophages, through chemical elements to remove foreign particles [52], [53]. Additionally, the growth factors and cytokines that stimulate the proliferation stage in the wound-healing process are excreted during this stage [52]. In contrast, the histological image of the wound treated with PVA/SA/Oil nanofiber shows a completed reconstruction of

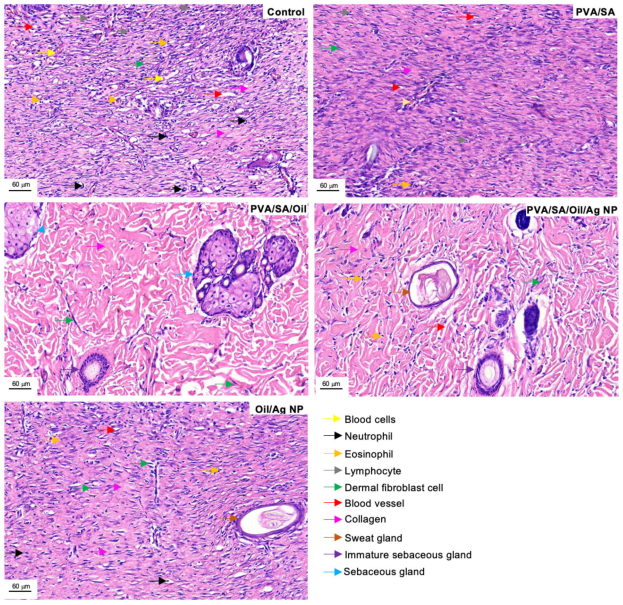

Fig. 11. Dermis layer of the wound zone in all the groups after H&E staining.

the skin. As Fig. 11 shows, not only collagen proteins, which are released by dermal fibroblast cells, but also new vessels, which supply nutrient components and oxygen to promote the regeneration and angiogenesis of granulation tissue, appeared densely in the dermis layer. In addition, the appearance of sebaceous glands indicated that the damaged skin was healing effectively. Moreover, fibroblast cells fully covered the dermis layer in the groups treated with the PVA/SA, PVA/SA/Oil, and Oil/Ag NP membranes. This phenomenon demonstrated that re-epithelialisation and wound contraction were occurring. Consequently, a mass of collagen fibres and endothelial cells were produced markedly to penetrate the wound zone. This stage can be defined as the proliferation phase of the healing process.

In a word, the histological results for all the treatment groups indicated the recovery of normal skin structure after 15 days. These results demonstrated that nanofiber membranes composed of PVA and SA with or without tamanu oil and nanosilver were capable of healing injured skin. Among these membranes, the PVA/SA/Oil nanofiber membrane was the best extracellular space for increasing the growth of factors, fibroblast cells, and endothelial cells in the healing stage.

IV. Conclusion

In this study, a series of antibacterial, antioxidant, and flexible nanofiber membranes based on PVA, SA, tamanu oil, and nanosilver was fabricated, and the membranes' morphological, mechanical, and biocompatible characteristics were evaluated. All the nanofiber membrane samples exhibited impressive liquid-absorption capabilities within 8 hours via swelling degree. Furthermore, these samples had not only high levels of antioxidant activity but also the capacity to inhibit *S. aureus* subsp. *aureus*. The cell-cytotoxicity results (*in vitro*) and the results of the animal-model tests (*in vivo*) testified to the membranes' good biocompatibility and wound-healing capacity. The pristine PVA/SA nanofiber with or without tamanu oil and nanosilver also promoted the healing of injured skin. The PVA/SA/Oil nanofiber membrane outperformed the others, achieving a healing percentage of over 98% within 15 days. This study identifies biomaterials that have the potential to improve wound-dressing applications.

Acknowledgment

The authors gratefully thank the BEing^2 Laboratory of the National Sun Yat-sen University for facilities and services.

References

[1] S. Guo and L. A. DiPietro, "Factors affecting wound healing," *J. Dental Res.*, vol. 89, no. 3, pp. 219–229, Feb. 2010, doi: 10.1177/0022034509359125.

[2] C. C. DeMerlis and D. R. Schoneker, "Review of the oral toxicity of polyvinyl alcohol (PVA)," *Food Chem. Toxicology*, vol. 41, no. 3, pp. 319–326, Mar. 2003, doi: 10.1016/s0278-6915(02)00258-2.

[3] A. M. Abd El-aziz, A. El-Maghraby, and N. A. Taha, "Comparison between polyvinyl alcohol (PVA) nanofiber and polyvinyl alcohol (PVA) nanofiber/hydroxyapatite (HA) for removal of Zn^{2+} ions from wastewater," *Arabian J. Chem.*, vol. 10, no. 8, pp. 1052–1060, Dec. 2017, doi: 10.1016/j.arabjc.2016.09.025.

[4] M. E. Okur, I. D. Karantas, Z. Şenyiğit, N. Ü. Okur, and P. I. Siafaka, "Recent trends on wound management: New therapeutic choices based on polymeric carriers," *Asian J. Pharmaceutical Sci.*, vol. 15, no. 6, pp. 661–684, Nov. 2020, doi: 10.1016/j.ajps.2019.11.008.

[5] M. Ding et al., "Antibacterial and hemostatic polyvinyl alcohol/microcrystalline cellulose reinforced sodium alginate breathable dressing containing *Euphorbiahumifusa* extract based on microfluidic spinning technology," *Int. J. Biol. Macromolecules*, vol. 239, Jun. 2023, Art. no. 124167, doi: 10.1016/j.ijbiomac.2023.124167.

[6] M. T. Manasa, K. V. Ramanamurthy, and P. A. Bhupathi, "Electrospun nanofibrous wound dressings: A review on chitosan composite nanofibers as potential wound dressings," *Int. J. Appl. Pharmaceutics*, vol. 15, no. 4, pp. 1–11, Jul. 2023, doi: 10.22159/ijap.2023v15i4.47912.

[7] F. Ijaz et al., "Biomolecules based hydrogels and their potential biomedical applications: A comprehensive review," *Int. J. Biol. Macromolecules*, vol. 253, Dec. 2023, Art. no. 127362, doi: 10.1016/j.ijbiomac.2023.127362.

[8] A. Aydin et al., "Biocompatible polyvinyl alcohol nanofibers loaded with amoxicillin and salicylic acid to prevent wound infections," *Biomed. Mater.*, vol. 18, no. 5, Sep. 2023, Art. no. 055029, doi: 10.1088/1748-605x/acf25c.

[9] H. S. Barakat, M. S. Freag, S. M. Gaber, A. Al Oufy, and O. Y. Abdallah, "Development of verapamil hydrochloride-loaded biopolymer-based composite electrospun nanofibrous mats: In vivo evaluation of enhanced burn wound healing without scar formation," *Drug Design, Develop. Therapy*, vol. 17, pp. 1211–1231, Apr. 2023, doi: 10.2147/dddt.s389329.

[10] M. M. Saraiva et al., "Alginate/polyvinyl alcohol films for wound healing: Advantages and challenges," *J. Biomed. Mater. Res. B, Appl. Biomaterials*, vol. 111, no. 1, pp. 220–233, Jan. 2023, doi: 10.1002/jbm.b.35146.

[11] S. Safi, M. Morshed, S. A. Hosseini Ravandi, and M. Ghiaci, "Study of electrospinning of sodium alginate, blended solutions of sodium alginate/poly(vinyl alcohol) and sodium alginate/poly(ethylene oxide)," *J. Appl. Polym. Sci.*, vol. 104, no. 5, pp. 3245–3255, Mar. 2007, doi: 10.1002/app.25696.

[12] J. B. Friday and D. Okano, "*Calophylluminophyllum* (kamani)," *Species Profiles Pacific Island agroforestry*, vol. 2, no. 1, pp. 1–17, Apr. 2006.

[13] P. Raharivelomanana et al., "Tamanu oil and skin active properties: From traditional to modern cosmetic uses," *OCL Oilseeds Fats Crops Lipids*, vol. 25, no. 5, Sep. 2018, doi: 10.1051/ocl/2018048.

[14] K. Tanoto, "Identification and flavonoids in ethanol-soluble *Calophylluminophyllum* oil from Indonesia," Indonesia Int. Inst. Life Sci., Tech. Rep. PHA 22-012;T202206118, Jul. 2022. [Online]. Available: http://repository.i3l.ac.id/jspui/handle/123456789/740

[15] S. S. Erdogan, T. F. Gur, N. K. Terzi, and B. Dogan, "Evaluation of the cutaneous wound healing potential of tamanu oil in wounds induced in rats," *J. Wound Care*, vol. 30, no. 9, pp. Vi–Vx, Sep. 2021, doi: 10.12968/jowc.2021.30.sup9a.v.

[16] D. S. Rodriguez, "Tamanu oil," *Aromatherapy J.*, no. 4, pp. 41–46, Apr. 2020.

[17] J.-L. Ansel et al., "Biological activity of polynesian *Calophylluminophyllum* oil extract on human skin cells," *Planta Medica*, vol. 82, nos. 11–12, pp. 961–966, Jun. 2016, doi: 10.1055/s-0042-108205.

[18] J. Zhou et al., "Electrospun Janus core (ethyl cellulose//polyethylene oxide) @ shell (hydroxypropyl methyl cellulose acetate succinate) hybrids for an enhanced colon-targeted prolonged drug absorbance," *Adv. Compos. Hybrid Mater.*, vol. 6, no. 6, pp. 1–16, Oct. 2023, doi: 10.1007/s42114-023-00766-6.

[19] D.-G. Yu and J. Zhou, "How can electrospinning further service well for pharmaceutical researches?" *J. Pharmaceutical Sci.*, vol. 112, no. 11, pp. 2719–2723, Nov. 2023, doi: 10.1016/j.xphs.2023.08.017.

[20] J. Zhou, P. Wang, D.-G. Yu, and Y. Zhu, "Biphasic drug release from electrospun structures," *Expert Opinion Drug Del.*, vol. 20, no. 5, pp. 621–640, May 2023, doi: 10.1080/17425247.2023.2210834.

[21] N. Tucker, J. J. Stanger, M. P. Staiger, H. Razzaq, and K. Hofman, "The history of the science and technology of electrospinning from 1600 to 1995," *J. Engineered Fibers Fabrics*, vol. 7, no. 2, Jun. 2012, Art. no. 155892501200702, doi: 10.1177/155892501200702s10.

[22] Y. Lang, B. Wang, M.-W. Chang, R. Sun, and L. Zhang, "Sandwich-structured electrospun pH-responsive dental pastes for anti-caries," *Colloids Surf. A, Physicochemical Eng. Aspects*, vol. 668, Jul. 2023, Art. no. 131399, doi: 10.1016/j.colsurfa.2023.131399.

[23] D. P. Ura, K. Berniak, and U. Stachewicz, "Critical length reinforcement in core-shell electrospun fibers using composite strategies," *Compos. Sci. Technol.*, vol. 211, Jul. 2021, Art. no. 108867, doi: 10.1016/j.compscitech.2021.108867.

[24] N. A. Norzain and W. C. Lin, "Orientated and diameter-controlled fibrous scaffolds fabricated using the centrifugal electrospinning technique for stimulating the behaviours of fibroblast cells," *J. Ind. Textiles*, vol. 51, no. 4, pp. 6728S–6752S, Jun. 2022, doi: 10.1177/1528083720988127.

[25] J. Chen et al., "Review of the principles, devices, parameters, and applications for centrifugal electrospinning," *Macromolecular Mater. Eng.*, vol. 307, no. 8, Aug. 2022, Art. no. 2200057, doi: 10.1002/mame.202200057.

[26] F. Müller, S. Jokisch, H. Bargel, and T. Scheibel, "Centrifugal electrospinning enables the production of meshes of ultrathin polymer fibers," *ACS Appl. Polym. Mater.*, vol. 2, no. 11, pp. 4360–4367, Oct. 2020, doi: 10.1021/acsapm.0c00853.

[27] S. M. H. Marjuban et al., "Recent advances in centrifugal spinning and their applications in tissue engineering," *Polymers*, vol. 15, no. 5, p. 1253, Mar. 2023, doi: 10.3390/polym15051253.

[28] H. Z. Luz and L. A. L. dos Santos, "Centrifugal spinning for biomedical use: A review," *Crit. Rev. Solid State Mater. Sci.*, vol. 48, no. 4, pp. 519–534, Jun. 2022, doi: 10.1080/10408436.2022.2080640.

[29] M. Koosha and H. Mirzadeh, "Electrospinning, mechanical properties, and cell behavior study of chitosan/PVA nanofibers," *J. Biomed. Mater. Res. Part A*, vol. 103, no. 9, pp. 3081–3093, Sep. 2015, doi: 10.1002/jbm.a.35443.

[30] D. K. Chandrasekharan, P. K. Khanna, T. V. Kagiya, and C. K. K. Nair, "Synthesis of nanosilver using a vitamin C derivative and studies on radiation protection," *Cancer Biotherapy Radiopharmaceuticals*, vol. 26, no. 2, pp. 249–257, Apr. 2011, doi: 10.1089/cbr.2010.0862.

[31] T. R. Sertbakan, E. K. Al-Shakarchi, and S. S. Mala, "The preparation of nano silver by chemical reduction method," *J. Modern Phys.*, vol. 13, no. 1, pp. 81–88, Jan. 2022, doi: 10.4236/jmp.2022.131006.

[32] D. E. Ermawati, D. S. Putro, and N. C. A. Susanto, "The characteristic and antibacterial activity of nanosilver biosynthetic using sweet orange," *J. Food Pharmaceutical Sci.*, vol. 11, no. 1, pp. 795–802, Mar. 2023, doi: 10.22146/jfps.5760.

[33] M. U. Rashid, M. K. H. Bhuiyan, and M. E. Quayum, "Synthesis of silver nano particles (Ag-NPs) and their uses for quantitative analysis of vitamin C tablets," *Dhaka Univ. J. Pharmaceutical Sci.*, vol. 12, no. 1, pp. 29–33, Sep. 2013.

[34] N. A. M. Razali and W.-C. Lin, "Accelerating the excisional wound closure by using the patterned microstructural nanofibrous mats/gentamicin-loaded hydrogel composite scaffold," *Mater. Today Bio*, vol. 16, Dec. 2022, Art. no. 100347, doi: 10.1016/j.mtbio.2022.100347.

[35] L. Cai et al., "Comparison of cytotoxicity evaluation of anticancer drugs between real-time cell analysis and CCK-8 method," *ACS Omega*, vol. 4, no. 7, pp. 12036–12042, Jul. 2019, doi: 10.1021/acsomega.9b01142.

[36] S. Kamiloglu, G. Sari, T. Ozdal, and E. Capanoglu, "Guidelines for cell viability assays," *Food Frontiers*, vol. 1, no. 3, pp. 332–349, Sep. 2020, doi: 10.1002/fft2.44.

[37] R. El Khoury, N. Nagiah, J. A. Mudloff, V. Thakur, M. Chattopadhyay, and B. Joddar, "3D bioprinted spheroidal droplets for engineering the heterocellular coupling between cardiomyocytes and cardiac fibroblasts," *Cyborg Bionic Syst.*, vol. 2021, Dec. 2021, Art. no. 9864212, doi: 10.34133/2021/9864212.

[38] F. B. Tessema, Y. H. Gonfa, T. B. Asfaw, M. G. Tadesse, and R. K. Bachheti, "Antioxidant activity of flavonoids and phenolic acids from dodonaea angustifolia flower: HPLC profile and PASS prediction," *J. Chem.*, vol. 2023, pp. 1–11, Mar. 2023, doi: 10.1155/2023/8315711.

[39] M. Muloiwa, S. Nyende-Byakika, and M. Dinka, "Comparison of unstructured kinetic bacterial growth models," *South Afr. J. Chem. Eng.*, vol. 33, pp. 141–150, Jul. 2020, doi: 10.1016/j.sajce.2020.07.006.

[40] M. Akhtar et al., "Centrifugal spinning of polyvinyl alcohol/sodium alginate-di-aldehyde-gelatin based antibacterial nanofibers intended for skin tissue engineering," *Mater. Lett.*, vol. 323, May 2022, Art. no. 132530, doi: 10.1016/j.matlet.2022.132530.

[41] J. Lei, A. McClelland, and T. H. Zeng, "Synthesis of silver nanoparticles by vitamin C for public health applications," in *Proc. IEEE 22nd Int. Conf. Nanotechnol. (NANO)*, Palma, Spain, Jul. 2022, pp. 488–491, doi: 10.1109/NANO54668.2022.9928735.

[42] S. Ahmed et al., "Oxymatrine loaded cross-linked PVA nanofibrous scaffold: Design and characterization and anticancer properties," *Macromolecular Biosci.*, vol. 23, no. 10, Oct. 2023, Art. no. 2300098, doi: 10.1002/mabi.202300098.

[43] X. Jiang, B. Zhou, and J. Wang, "Super-wetting and self-cleaning polyvinyl alcohol/sodium alginate nanofiber membrane decorated with MIL-88A(Fe) for efficient oil/water emulsion separation and dye degradation," *Int. J. Biol. Macromolecules*, vol. 253, Dec. 2023, Art. no. 127205, doi: 10.1016/j.ijbiomac.2023.127205.

[44] P. K. Tyagi et al., "Ascorbic acid and polyphenols mediated green synthesis of silver nanoparticles from *Tageteserecta* L. Aqueous leaf extract and studied their antioxidant properties," *J. Nanomaterials*, vol. 2021, pp. 1–9, Aug. 2021, doi: 10.1155/2021/6515419.

[45] M. Barbalinardo et al., "Surface properties modulate protein corona formation and determine cellular uptake and cytotoxicity of silver nanoparticles," *Nanoscale*, vol. 13, no. 33, pp. 14119–14129, Aug. 2021, doi: 10.1039/d0nr08259g.

[46] S. Sellimi et al., "Structural, physicochemical and antioxidant properties of sodium alginate isolated from a Tunisian Brown seaweed," *Int. J. Biol. Macromolecules*, vol. 72, pp. 1358–1367, Jan. 2015, doi: 10.1016/j.ijbiomac.2014.10.016.

[47] M. Cassien et al., "Improving the antioxidant properties of *Calophylluminophyllum* seed oil from French polynesia: Development and biological applications of resinous ethanol-soluble extracts," *Antioxidants*, vol. 10, no. 2, p. 199, Jan. 2021, doi: 10.3390/antiox10020199.

[48] L. Bertino, F. Guarneri, S. P. Cannavò, M. Casciaro, G. Pioggia, and S. Gangemi, "Oxidative stress and atopic dermatitis," *Antioxidants*, vol. 9, no. 3, p. 196, Feb. 2020, doi: 10.3390/antiox9030196.

[49] L. J. Bessa, P. Fazii, M. Di Giulio, and L. Cellini, "Bacterial isolates from infected wounds and their antibiotic susceptibility pattern: Some remarks about wound infection," *Int. Wound J.*, vol. 12, no. 1, pp. 47–52, Feb. 2013, doi: 10.1111/iwj.12049.

[50] T. Léguillier et al., "The wound healing and antibacterial activity of five ethnomedical *Calophylluminophyllum* oils: An alternative therapeutic strategy to treat infected wounds," *PLoS ONE*, vol. 10, no. 9, Sep. 2015, Art. no. e0138602, doi: 10.1371/journal.pone.0138602.

[51] M. Abbasi et al., "An intriguing approach toward antibacterial activity of green synthesized Rutin-templated mesoporous silica nanoparticles decorated with nanosilver," *Sci. Rep.*, vol. 13, no. 1, p. 5987, Apr. 2023, doi: 10.1038/s41598-023-33095-1.

[52] J. M. Reinke and H. Sorg, "Wound repair and regeneration," *Eur. Surgical Res.*, vol. 49, no. 1, pp. 35–43, Aug. 2012, doi: 10.1159/000339613.

[53] S. A. Eming, P. Martin, and M. Tomic-Canic, "Wound repair and regeneration: Mechanisms, signaling, and translation," *Sci. Transl. Med.*, vol. 6, no. 265, p. 265, Dec. 2014, doi: 10.1126/scitranslmed.3009337.